Hindawi Publishing Corporation
International Journal of Photoenergy
Volume 2014, Article ID 570506, 8 pages
http://dx.doi.org/10.1155/2014/570506

Research Article

Potential Use of C_{60}/2-Hydroxypropyl-β-cyclodextrin Nanoparticles as a New Photosensitizer in the Treatment of Cancer

Abdulmalik Altaf,[1,2] Hibah Aldawsari,[1] Zainy M. Banjar,[1] Daisuke Iohara,[3] Makoto Anraku,[3] Kaneto Uekama,[1,4] and Fumitoshi Hirayama[3]

[1] *Faculty of Pharmacy, King Abdulaziz University, Jeddah 21589, Saudi Arabia*
[2] *Faculty of Medicine, King Abdulaziz University, Jeddah 21589, Saudi Arabia*
[3] *Faculty of Pharmaceutical Sciences, Sojo University, 4-22-1 Ikeda, Kumamoto 860-0082, Japan*
[4] *DDS Research Institute, Sojo University, 4-22-1 Ikeda, Kumamoto 860-0082, Japan*

Correspondence should be addressed to Fumitoshi Hirayama; fhira@ph.sojo-u.ac.jp

Received 23 October 2013; Revised 16 December 2013; Accepted 26 December 2013; Published 13 February 2014

Academic Editor: Victor Loschenov

The photosensitizing ability of C_{60}/2-hydroxypropyl-β-cyclodextrin (HP-β-CyD) nanoparticles under visible light irradiation was studied by electron spin resonance (ESR) and phototoxicity on cancer cells. In addition, the photoinduced antitumor effect to the tumor-bearing mice was evaluated. C_{60} nanoparticles were prepared by grinding a mixture of HP-β-CyD. The resulting C_{60}/HP-β-CyD nanoparticles were highly-sensitive to visible light and generated higher levels of $^1O_2$ than protoporphyrin IX (PpIX). C_{60}/HP-β-CyD reduced the viability of cancer cells (HeLa cells and A549 cells) in response to irradiation by visible light in a dose-dependent manner. The IC_{50} values of the C_{60}/HP-β-CyD nanoparticles was 10 μM for HeLa cells and 60 μM for A549 cells at an irradiation level of 35 mW/cm^2. The photodynamic effect of C_{60}/HP-β-CyD nanoparticles on the *in vivo* growth of mouse sarcoma S-180 cells was evaluated after intratumor injection. The outcome of PDT by C_{60}/HP-β-CyD was directly dependent on the dose of irradiated light. Treatment with C_{60}/HP-β-CyD nanoparticles at a C_{60} dose of 2.0 mg/kg under visible light irradiation at 350 mW/cm^2 (63 J/cm^2) markedly suppressed tumor growth, whereas that at 30 J/cm^2 was less effective. These findings suggest that C_{60}/HP-β-CyD nanoparticles represent a promising candidate for use in cancer treatment by PDT.

1. Introduction

Photodynamic therapy (PDT), which involves the production of reactive oxygen species (ROS), is a next-generation cancer treatment. In PDT, a photosensitizer is systemically administered, either locally or topically, and tumor sites are then irradiated by visible light to site-selectively generate ROS, leading to cell death and tissue destruction [1–3]. Therefore, PDT is an effective method for destroying diseased tissues without damaging surrounding healthy tissue. The ideal photosensitizer for use in PDT should meet the following requirements: (1) have high quantum yields for generating ROS, (2) have a strong absorbance with a high extinction coefficient in the long-wavelength (600~800 nm) region, where the maximum penetration of tissue by the penetrating light occurs [4], and (3) have minimal toxicity under conditions of nonlight irradiation. Many of the currently clinically employed photosensitizers are based on porphyrin molecules such as Photofrin, a hematoporphyrin derivative, and 5-aminolevulinic acid (ALA), a precursor of protoporphyrin IX (PpIX). However, these compounds have several disadvantages such as suboptimal tumor selectively and poor light penetration into tumors due to the absorption of the relatively short wavelengths. Therefore, more efficient photosensitizers are currently in various stages of development [5].

Fullerenes are currently of great interest for practical applications that take advantage of their unique electronic

properties and biological activities [6–8]. The fullerene family, especially C_{60}, is generally regarded as an efficient photosensitizer for PDT [9] due to light absorption at relatively long wavelengths and the high quantum yield of photoexcitation reactions [10, 11]. C_{60} molecules generate ROS such as singlet oxygen ($^1O_2$) and superoxide anion radicals ($O_2^{\bullet-}$) under light irradiation [10, 12]. In a previous study, we reported on the preparation of stable C_{60} nanoparticles (mean particle size ca. 90 nm), the surfaces of which were covered by hydrophilic 2-hydroxypropyl-β-cyclodextrin (HP-β-CyD) through physical adsorption and weak hydrophobic interactions [13]. The C_{60}/HP-β-CyD nanoparticles showed cell toxicity due to their ability to generate ROS when irradiated with visible light [14]. However, few studies have focused on the *in vivo* photodynamic activity of C_{60}. In spite of the advantages of PDT over conventional therapies, PDT is not extensively used, compared to the well-established chemo- and radiotherapy due to insufficient understanding of the procedures involved. In particular, the outcome of PDT is influenced by several factors such as the dose of the photosensitizer used, the presence of molecular oxygen, the irradiation time and the interval between drug administration and irradiation, and the correct dose of light. Thus, it is necessary to validate standard protocols for each individual photosensitizer in order to obtain an effective and reliable outcome [15]. In this study, we evaluated the photosensitizing ability of C_{60}/HP-β-CyD nanoparticles under visible light irradiation as a new photosensitizer in PDT. In addition, we examined the *in vivo* photodynamic activity of C_{60}/HP-β-CyD nanoparticles in tumor-bearing mice after visible light irradiation.

2. Materials and Methods

2.1. Materials. C_{60} (nanom purple SUH) was purchased from Frontier Carbon Co. (Tokyo, Japan). 2-Hydroxypropyl-β-CyD (HP-β-CD, degree of substitution (D.S.) of the 2-hydroxypropyl group was 5.6) was a gift from Nihon Shokuhin Kako Co., Ltd. (Tokyo, Japan). Hydrophilic C_{60}/HP-β-CyD nanoparticles were prepared by the coground method reported in previous paper [13]. ALA was purchased from Wako Pure Chemical Industries Ltd. (Tokyo, Japan). PpIX disodium salt was purchased from Sigma-Aldrich Co. LLC. (Tokyo, Japan) and dissolved in 10 mM NaOH or 10% dimethyl sulfoxide (DMSO) for ESR study and cell toxicity study, respectively. 5,5-Dimethyl-1-pyrroline N-oxide (DMPO) was purchased from Labotec Co. Ltd. (Tokyo, Japan). 4-Hydroxy-2,2,6,6,-tetramethylpiperidine (TEMP-OH) was purchased from Wako Pure Chemical Industries Ltd. (Tokyo, Japan). Eagle's minimum essential medium (MEM), Dulbecco's modified Eagle's medium (DMEM), and penicillin-streptomycin were purchased from GIBCO Invitrogen Co. (Tokyo, Japan). Fetal calf serum (FCS) was obtained from Nichirei (Tokyo, Japan). All other materials and solvents were of analytical reagent grade and Milli-Q water was used throughout the study.

2.2. Photosensitizing Ability of C_{60}/HP-β-CyD Nanoparticles under Visible Light Irradiation. The generation of $O_2^{\bullet-}$ and $^1O_2$ from C_{60}/HP-β-CyD nanoparticles and PpIX were measured using an X-band electron spin resonance (ESR) spectrometer (JES-FA100, JEOL Ltd., Tokyo, Japan) under the following conditions: microwave frequency 9.417 GHz, microwave power 4 mW, field modulation 0.1 mT at 100 kHz, and sweep time 30 s. $O_2^{\bullet-}$ was detected using DMPO as a spin-trapping reagent. The DMPO-OH signal was detected on ESR spectra, because the unstable DMPO-OOH adduct was rapidly converted to a DMPO-OH adduct. One hundred microliter aliquots of sample solutions and 80 μL of Milli-Q and 20 μL of DMPO were mixed well under aerobic conditions. $^1O_2$ was also detected by the ESR using TEMP-OH as a spin-trapping reagent. One hundred microliters of a sample solution and 100 μL of TEMP-OH (160 mM) were well mixed under aerobic conditions. The mixed solutions were collected in a flat cell, then exposed to visible light generated by a xenon light source (MAX-303, Asahi spectra Co., Ltd., Tokyo, Japan), and subjected immediately to ESR measurement. Generation efficiency of $O_2^{\bullet-}$ and $^1O_2$ was evaluated by the relative intensity to an external reference of Mn^{2+}.

2.3. Photoinduced Cell Toxicity by C_{60}/HP-β-CyD Nanoparticles. HeLa cells were cultured in MEM containing 100 units/mL penicillin-streptomycin, supplemented with 10% fetal bovine serum at 37°C and 5% of CO_2. A549 cells were cultured in DMEM containing 100 units/mL penicillin-streptomycin, supplemented with 10% fetal bovine serum at 37°C and 5% of CO_2. The cells were seeded in 96-well plates at a density of 2.0×10^4 cells/well for HeLa cells and 1.0×10^4 cells/well in the case of A549 cells. After growing overnight, the cells were incubated with the samples (1 μM~150 μM for C_{60} and 1 μM~300 μM for ALA) for 24 h in the dark. The cells were washed with phosphate-buffered saline (PBS) and replaced with fresh culture medium. The treated cells were exposed to light (35 mW/cm^2, 400–700 nm) for 30 min, using a xenon light source. To measure the viability of cells as a ratio (%) compared with cells which were not treated with the samples, a WST-1 (4-[3-(4-iodophenyl)-2-(4-nitrophenyl)-2*H*-5-tetrazolio]-1,3-benzene disulfonate) assay was carried out 24 h after the photoirradiation, by using a Cell Counting Kit (Dojindo Laboratories, Kumamoto, Japan). WST-1 works by reacting with the mitochondrial succinate-tetrazolium reductase forming the formazan dye. The effect of ROS scavengers on cell viability was studied used HeLa cells. The cells were incubated with C_{60}/HP-β-CyD nanoparticles for 24 h and then washed with PBS and the medium was replaced with fresh medium including 10 mM of L-histidine, 2,5-dimethylfuran (DMF) and 1,4-diazabicyclo [2, 2, 2] octane (DABCO) or 500 unit/mL of superoxide dismutase (SOD). After 1 h incubation, the treated cells were exposed to the light. To measure the viability of cells, WST-1 assay was carried out 24 h after the photoirradiation.

2.4. In Vivo Photodynamic Activity of C_{60}/HP-β-CyD Nanoparticles. The care and maintenance of animals were conducted in accordance with the institutional guidelines of the Institutional Animal Care and Use Committee of Sojo

University. To prepare a mouse tumor model, mouse sarcoma S-180 cells were acclimatized to the *in vivo* conditions by intraperitoneal growth in ddY mice (Kyudo Co. Ltd., Saga, Japan). The cells were implanted by subcutaneous injection in the dorsal skin of 6-week-old ddY mice (2×10^7 cells/mL, 100 μL/mouse). When the tumor mass reached a diameter of 7~8 mm, 0.1 mL of C_{60}/HP-β-CyD nanoparticles in 5% glucose solution (C_{60} = 1 mM) were injected to the intratumor (2.0 mg/kg of C_{60}, i.e., 0.072 mg of C_{60} per 35 ± 2 g body weight). The tumor tissue was exposed to visible light from a xenon light source at 400~700 nm (100~350 mW/cm^2). Tumor volume (mm^3) was calculated as $(W^2 \times L)/2$ by measuring the length (L) and width (W) of the tumor on the dorsal skin.

3. Results and Discussion

3.1. Photosensitizing Ability of C_{60}/HP-β-CyD Nanoparticles under Visible Light Irradiation. C_{60} is generally regarded to be an effective photosensitizer for PDT [9]; however, its extremely low solubility and poor dispersibility in water have significantly impeded pharmaceutical applications [16, 17]. Although several water soluble fullerene derivatives have been produced and their photodynamic activity evaluated [18, 19], only few studies in which the efficacy of C_{60} was compared with other photosensitizers have appeared. We therefore examined the *in vitro* photosensitizing ability of C_{60}/HP-β-CyD nanoparticles, in comparison with that of PpIX by means of an ESR spin-trapping method. A xenon light source was used to produce homogenous light in the visible light range (Supplementary Figure 1(S) in Supplementary Material available online at http://dx.doi.org/10.1155/2014/570506). Figure 1(a) shows ESR spectra of C_{60}/HP-β-CyD colloidal and PpIX solutions under photoirradiation. These photosensitizers produced three characteristic signals for TEMPO-OH in ESR spectra [20], indicating that $^1O_2$ was generated by the photoirradiation. The relative intensity of the TEMPO-OH to an external reference (Mn^{2+}) in these solutions increased with the photoirradiation time (Figure 1(b)). C_{60}/HP-β-CyD nanoparticles generated higher levels of $^1O_2$ than PpIX at every time period of photoirradiation. As shown in Figure 1(c), the generation of $^1O_2$ from these photosensitizers was almost the same as that produced under low light energy (5 mW/cm^2); however, the C_{60}/HP-β-CyD nanoparticles were highly sensitive to the power of the light and large amounts of $^1O_2$ were generated when a higher energy light source was used. It was estimated that at least 1.5 times larger energy is needed for PpIX to generate the same amount of $^1O_2$ as that produced in the case of a C_{60} colloidal solution. For both C_{60}/HP-β-CyD and PpIX, the generation of $^1O_2$ under visible light irradiation was concentration dependent (Figure 1(d)). The generation of $^1O_2$ at a low concentration (20 μM) was low in both the C_{60} and PplX systems, whereas C_{60}/HP-β-CyD showed higher generation ability in the higher concentration range compared with that for PpIX. We previously reported that the HP-β-CyD-enhanced generation of $^1O_2$ was due to the partial deposition of C_{60} in the hydrophobic CyD cavity [13], because the production of $^1O_2$ shows a preference for nonpolar solvents. The low generation of $^1O_2$ at low concentrations may be due to the dissociation of HP-β-CyD from the C_{60} nanoparticles. These collective results indicate that C_{60}/HP-β-CyD has a potent photosensitizing ability when compared with PpIX under visible light irradiation. In addition, C_{60} has capability to generate $O_2^{\bullet -}$ when irradiated with visible light, as shown in Figure 2. A four-line ESR signal corresponding to DMPO-OH was detected in the ESR spectra [21], suggesting that $O_2^{\bullet -}$ is generated in the C_{60}/HP-β-CyD colloidal solution. On the other hand, such a signal was not observed for PpIX. The generation of $O_2^{\bullet -}$ by C_{60}/HP-β-CyD was also light power dependent and dose dependent, similar to that for the generation of $^1O_2$ (Figure 1). C_{60}/HP-β-CyD showed the higher absorption than that of PpIX at the region of 420 nm~540 nm and almost the same absorption spectra at the region of 600~700 nm where the maximum light absorption of C_{60} occurred at 620 nm, while that of PpIX was at 635 nm (Supplementary Figure 1(S)). The quantum yield for $^1O_2$ at this wavelength was reported to be 0.96 for C_{60} in benzene [10], while the corresponding value was 0.56 for PpIX in phosphate buffer, the former value being higher than those for Photofrin and other photosensitizers [22, 23]. In this study, constant light energy was supplied in the wavelength range of 400~700 nm. Therefore, the different ROS generation ability of C_{60} and PpIX is probably due to not only the higher absorption at blue region but also the difference in the intrinsic photoexcitation properties of the photosensitizers. Further, it is known that extensive aggregation of photosensitizers significantly accelerates the decay of the excited triplet state [24], thus reducing the photosensitizing ability. In a previous study, we reported that C_{60} exists in the form of stable small aggregates with a particle size ca.90 nm in C_{60}/HP-β-CyD colloidal solutions [13]. This might explain the higher photosensitizing ability of colloidal solutions of C_{60}/HP-β-CyD, compared to PpIX solutions.

3.2. Photoinduced Cell Toxicity by C_{60}/HP-β-CyDs Nanoparticles. The photodynamic activity of C_{60}/HP-β-CyD nanoparticles on human cervical cancer HeLa cells and human lung carcinoma A549 cells was evaluated by WST-1 assays. We chose ALA as a control photosensitizer because PpIX is administered clinically in the form of a precursor. ALA is a naturally occurring amino acid that endogenously produced PpIX and the resulting PpIX can generate singlet oxygen leading to cancer cell death. The use of ALA has become a widely acceptable and popular procedure, particularly for the treatment of skin cancer [25]. As shown in Figure 3, C_{60}/HP-β-CyD nanoparticles and ALA reduced the viability of these cells in response to the visible light irradiation and in a dose-dependent manner. The IC_{50} value of ALA for HeLa and A549 cells was 100 μM and 150 μM, respectively. In the case of C_{60}/HP-β-CyD nanoparticles, the cellular survival significantly decreased at lower concentrations of C_{60} as a result of the photoirradiation. The IC_{50} value of the C_{60}/HP-β-CyD nanoparticles was 10 μM for HeLa cells and 60 μM for A549 cells, which were much lower than those of ALA.

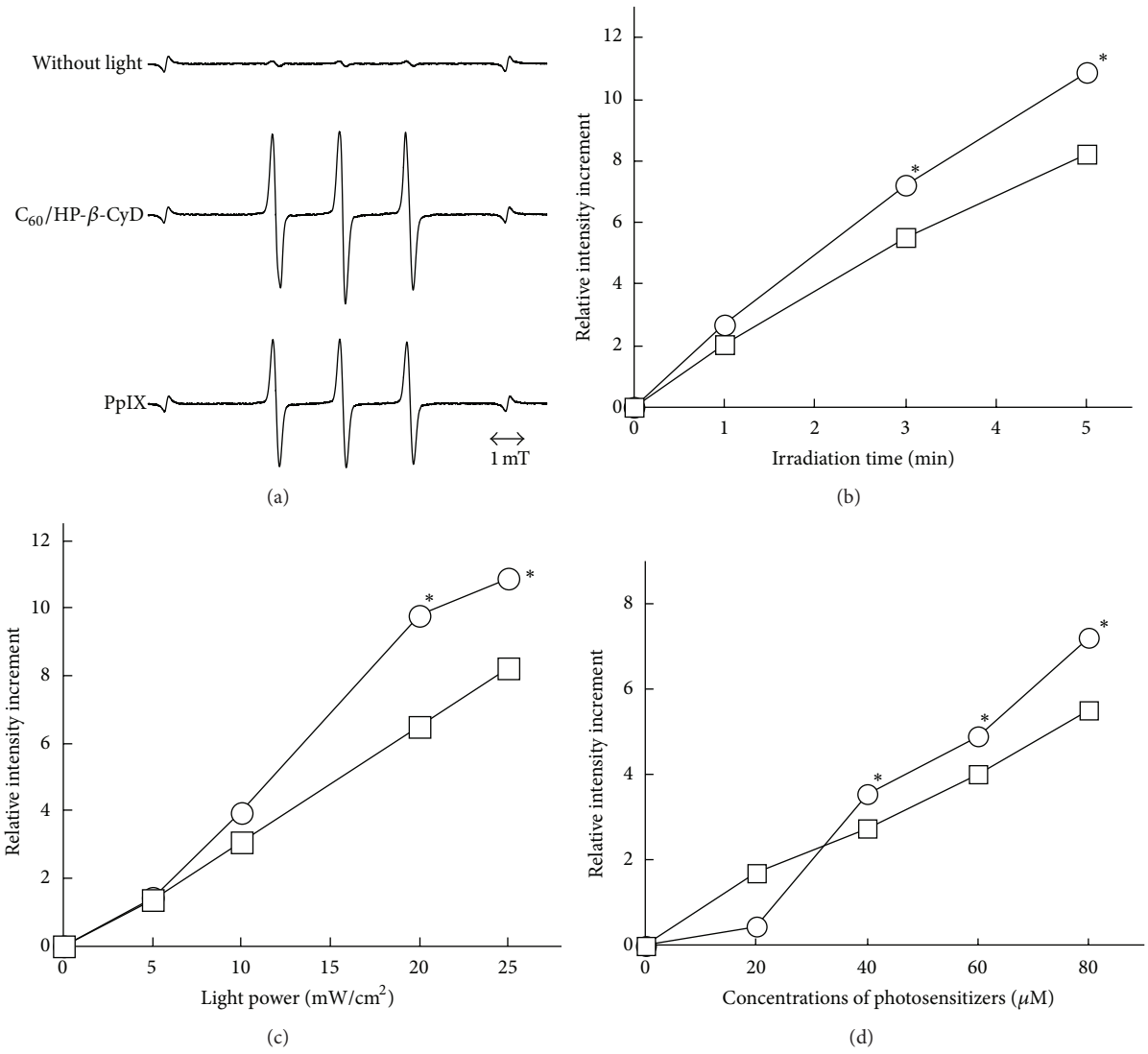

Figure 1: ESR spectra of the TEMPO-OH adduct generated in a C_{60}/HP-β-CyD colloidal solution and a PpIX solution (C_{60} and PpIX = 80 μM, light irradiation at 25 mW/cm^2 for 5 min) (a). Its relative intensity increment after visible light irradiation. (b) Effects of the light power (c) and concentrations of photosensitizers (d) on the generation of $^1O_2$. Empty circle: C_{60}/HP-β-CyD nanoparticles; empty square: PpIX. Each point represents the mean ± S.E. of 3 experiments.* $P < 0.05$ versus PpIX.

This is probably due to the great ROS generation of C_{60}/HP-β-CyD nanoparticles compared with ALA. When the cell viability test was conducted in the dark, no cell toxicity was observed at these concentrations of photosensitizers. In addition, C_{60}/HP-β-CyD nanoparticles have capability to generate $O_2^{\bullet-}$ when irradiated with visible light as described above. In this study, the extracellular C_{60} was washed away prior to light irradiation; therefore, ROS such as $O_2^{\bullet-}$ and $^1O_2$ might be generated from C_{60} taken up by cells, leading to the cell death. To assess the contribution of $O_2^{\bullet-}$ and $^1O_2$ to the cell death, the effects of $^1O_2$ scavengers, such as L-histidine, 2,5-dimethylfuran (DMF) and 1,4-diazabicyclo [2, 2, 2] octane (DABCO) [20] and $O_2^{\bullet-}$ specific scavenger, superoxide dismutase (SOD), were studied. As shown in Figure 4, cell viability was increased by the addition of these ROS scavengers. These results indicate that both $O_2^{\bullet-}$ and $^1O_2$ contribute to the potent photoinduced cell toxicity of C_{60}/HP-β-CyD nanoparticles. However, we could not discuss which ROS is more effective to the cell death because the scavenging ability and cellular permeability of these scavengers were different from each other. Also, the amounts of C_{60} and ALA (or PpIX produced in the cells), especially C_{60}, taken up in the cells could not be measured accurately due to the UV detection limit. The present results clearly indicate that C_{60}/HP-β-CyD nanoparticles are toxic to cells only when irradiated by visible light, although further study is still needed to precisely evaluate the differences of the photosensitizers, C_{60} and ALA.

3.3. In Vivo Photodynamic Activity of C_{60}/HP-β-CyD Nanoparticles. Since C_{60}/HP-β-CyD nanoparticles demonstrated a potential to succeed as photosensitizer in PDT, a subsequent *in vivo* study was conducted to determine the standard

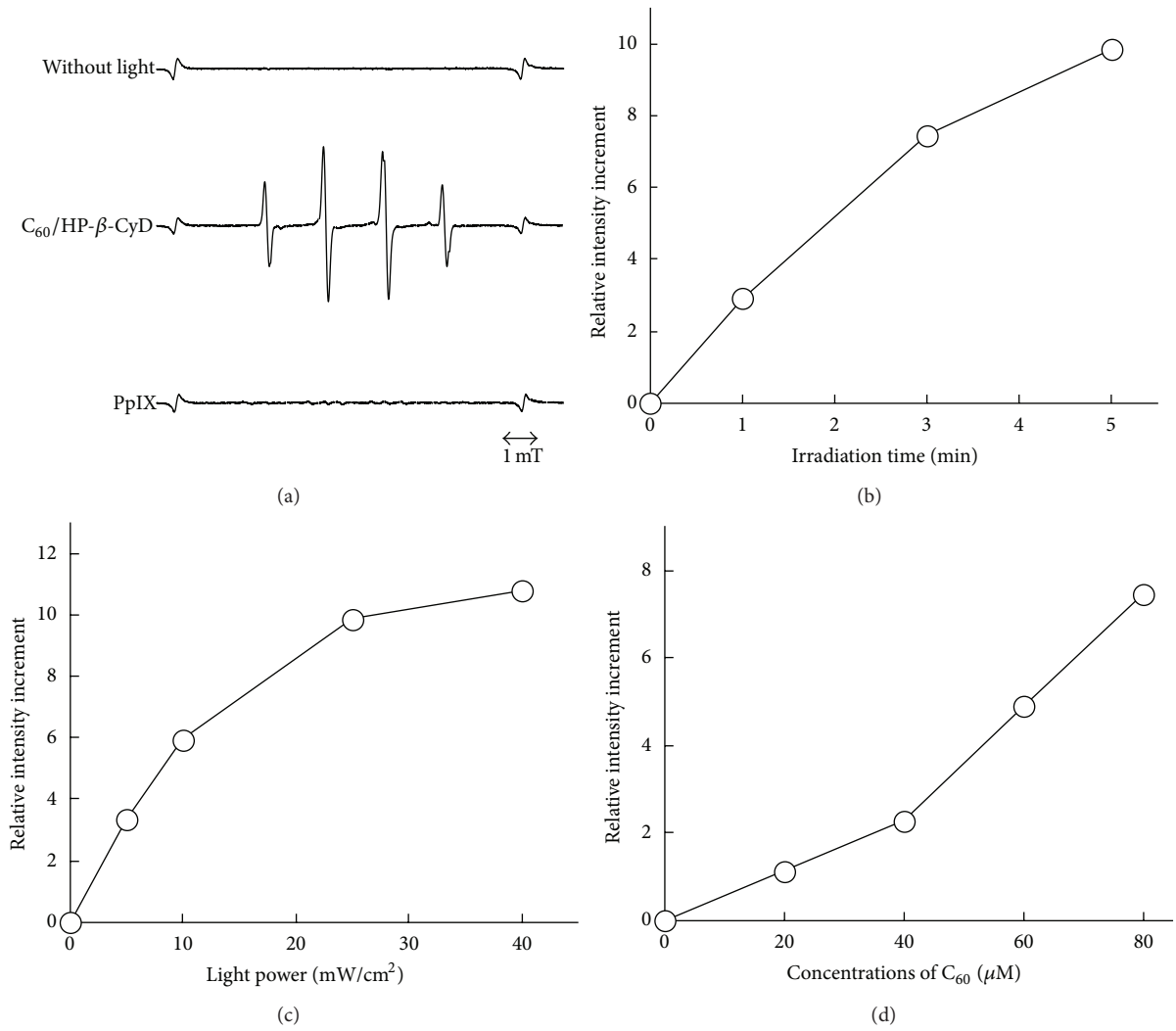

FIGURE 2: ESR spectra of the DMPO-OH adduct generated in the C_{60}/HP-β-CyD colloidal solution (C_{60} = 40 μM, light irradiation at 40 mW/cm^2 for 5 min) (a). Its relative intensity increment after visible light irradiation (b). Effects of the light power (c) and concentrations of photosensitizers (d) on the generation of $O_2^{\bullet -}$. Each point represents the mean ± S.E. of 3 experiments.

protocols for the effective application of PDT by C_{60}. Figure 5 shows the photodynamic effect of C_{60}/HP-β-CyD nanoparticles on the *in vivo* growth of mouse sarcoma S-180 cells after intratumor injection. The tumor was irradiated for a short time period which was repeated at 30 s intervals. The tumor growth was similar to that observed for a saline injection, when treated with C_{60}/HP-β-CyD nanoparticles at a C_{60} dose of 2.0 mg/kg, followed by visible light irradiation once at 100 mW/cm^2 for 300 s (30 J/cm^2) or 5 times at 200 mW/cm^2 for 60 s (total light does 60 J/cm^2). On the other hand, it was significantly suppressed when the irradiation power was increased, that is, 5 times at 250 mW/cm^2 for 60 s (total light does 75 J/cm^2). However, light irradiation alone at 75 J/cm^2 significantly affected the tumor growth, as shown by the symbol of the empty triangle in Figure 5. In fact, the temperature increased to 50°C from 37°C when a mercury thermometer was directly light-irradiated at 250 W/cm^2 for 60 s and normal skin was burned after being irradiated at this power. Therefore, it is very important to choose adequate irradiation doses to avoid damage to healthy tissues caused by a temperature increase. Figure 6 shows the photodynamic effects of C_{60}/HP-β-CyD nanoparticles on tumor growth as the result of visible light irradiation 12 times at 350 mW/cm^2 for 15 s (total light dose 63 J/cm^2). As shown in Figures 6(a) and 6(b), tumor growth was significantly suppressed by this treatment at a dose of 2.0 mg/kg C_{60}/HP-β-CyD. The treatment with C_{60}/HP-β-CyD at a dose of 0.4 mg/kg was less effective against tumor growth, when compared with a dose of 2.0 mg/kg. The light irradiation alone had no effect on tumor growth and there was no significant difference compared with the saline injected group, suggesting a minor hyperthermia of the irradiation alone in this condition. The time profile for mice tumor growth treated with C_{60}/HP-β-CyD nanoparticles without light irradiation was similar to that for the saline injection. Thus, C_{60}/HP-β-CyD itself had no detectable cytocidal effect on the tumor tissue in the

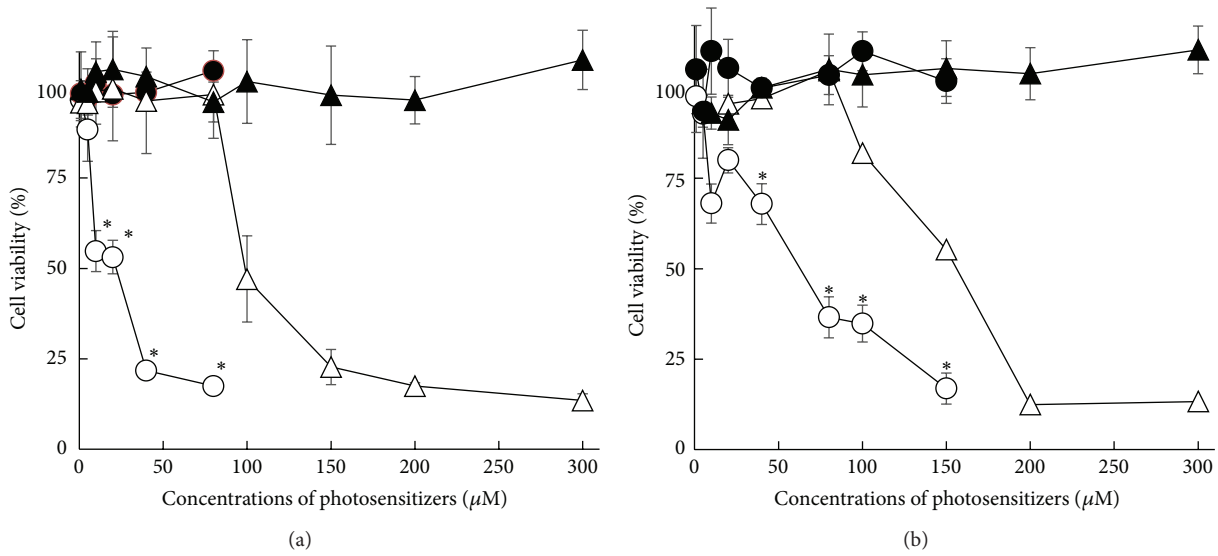

Figure 3: Photodynamic activities of C_{60}/HP-β-CyD nanoparticles and ALA for HeLa cells (a) and A549 cells (b) after visible light irradiation at 35 mW/cm^2. Black filled circle: C_{60}/HP-β-CyD in the dark; black filled triangle: ALA in the dark; empty circle: C_{60}/HP-β-CyD with light irradiation; empty triangle: ALA with light irradiation. Each value points the mean ± S.E. of 3–5 experiments. $^*P < 0.05$ versus ALA with light irradiation.

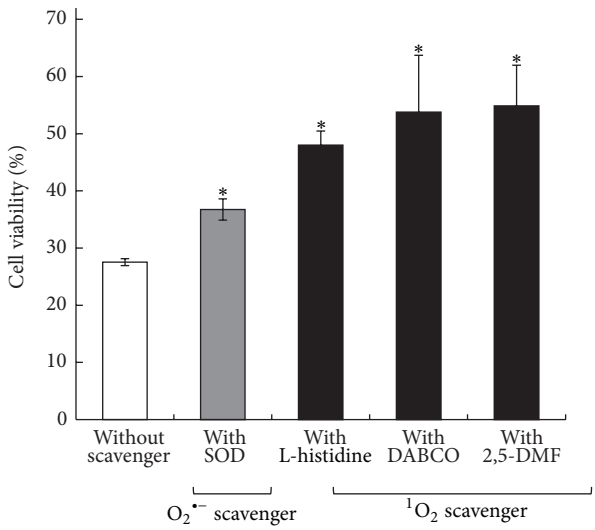

Figure 4: Effect of ROS scavengers on photodynamic effect by C_{60}/HP-β-CyD nanoparticles on HeLa cells. Each value represents the mean ± S.E. of 5 experiments. $^*P < 0.05$ versus without ROS scavenger.

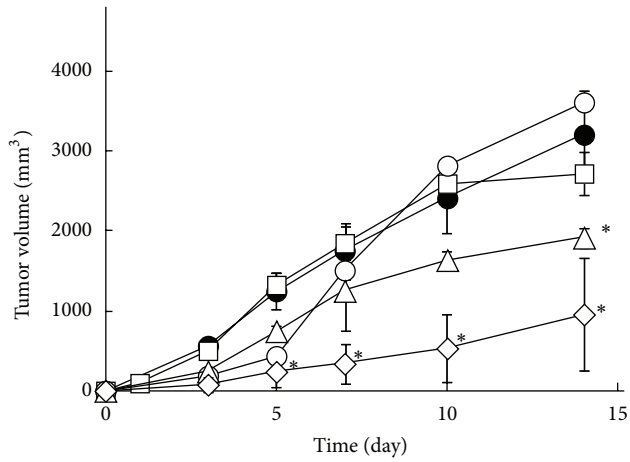

Figure 5: Photodynamic effects of C_{60}/HP-β-CyD nanoparticles (C_{60} = 2.0 mg/kg) on tumor growth after intratumor injection to the tumor-bearing mice plus light irradiation. Black filled circle: saline; empty square: C_{60}/HP-β-CyD plus light irradiation (30 J/cm^2); empty circle: C_{60}/HP-β-CyD plus light irradiation (60 J/cm^2); empty lozenge: C_{60}/HP-β-CyD plus light irradiation (75 J/cm^2); empty triangle: saline plus light irradiation (75 J/cm^2). Each point represents the mean ± S.E. of 3–9 experiments. $^*P < 0.05$ versus saline.

absence of irradiation. At this power, the temperature rise was within 5°C for 15 s and no light-induced skin damage was observed. It is interesting to note that the photodynamic effect was completely different depending on the protocol of light irradiation, even though the light energy supplied to tumor was almost the same (60 J/cm^2 in Figure 5 and 63 J/cm^2 in Figure 6). These results indicate that the PDT effect mainly depends on total light doses. Another parameter that limits tumor cell kill is the availability of oxygen in the tissue undergoing PDT treatment [26]. Since ROS arises from ground state oxygen, this process consumes oxygen in the tissue environment. The repeated intervals in the treatment at 63 J/cm^2 might allow to oxygen to be regenerated and for a constant oxygen level to be maintained during PDT [27], leading to a sufficient PDT effect. Therefore, efficient PDT using C_{60} can be achieved by the repeated, short periods of high power irradiation. As shown in Figure 6(c),

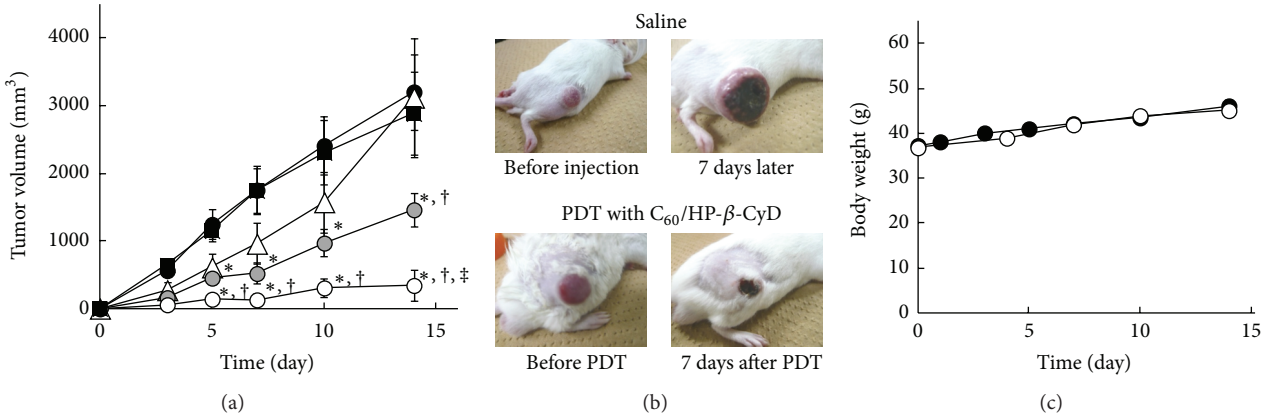

FIGURE 6: Photodynamic effects of C_{60}/HP-β-CyD nanoparticles on tumor growth (a). Appearances of tumor (b) and changes in body weight (c) after intratumor injection to the tumor-bearing mice plus light irradiation. Black filled circle: saline; black filled square: C_{60}/HP-β-CyD; empty triangle: saline plus light irradiation (63 J/cm^2); shadowed circle: C_{60}/HP-β-CyD (0.4 mg/kg) plus light irradiation (63 J/cm^2); empty circle: C_{60}/HP-β-CyD (2.0 mg/kg) plus light irradiation (63 J/cm^2). Each point represents the mean ± S.E. of 6–9 experiments. $^*P < 0.05$ versus saline. $^\dagger P < 0.05$ versus saline plus light irradiation. $^\ddagger P < 0.05$ versus C_{60}/HP-β-CyD (0.4 mg/kg) plus light irradiation (63 J/cm^2).

no significant difference in change of body weight was observed between C_{60}/HP-β-CyD nanoparticles and the saline solution injected mice, suggesting that the C_{60}/HP-β-CyD nanoparticles are relatively nontoxic. The light dose supplied in this experiment was not as high as the clinically used dose of 60~200 J/cm^2 from a laser [15, 28]. Therefore, C_{60}/HP-β-CyD nanoparticles appear to have great potential for use as a new photosensitizer for cancer treatment in PDT.

4. Conclusion

We investigated the potency of C_{60}/HP-β-CyD nanoparticles as a new photosensitizer in the treatment of cancer. C_{60}/HP-β-CyD nanoparticles had substantial photosensitizing ability compared with PpIX for the generation of $^1O_2$ under visible light irradiation. In addition, C_{60}/HP-β-CyD nanoparticles were capable of generating $O_2^{\bullet-}$ under visible light irradiation. The IC_{50} value of the C_{60}/HP-β-CyD nanoparticles under photoirradiation was 10 μM for HeLa cells and 60 μM for A549 cells at an irradiation level of 35 mW/cm^2. Efficient PDT using C_{60}/HP-β-CyD nanoparticles in tumor-bearing mice was achieved by a treatment with C_{60}/HP-β-CyD nanoparticles at a C_{60} dose of 2.0 mg/kg followed by 12 periods of visible light irradiation at 350 mW/cm^2 for 15 s (total light dose 63 J/cm^2). These results demonstrate that C_{60}/HP-β-CyD nanoparticles are promising candidates for cancer treatment by PDT. The accumulation of C_{60} in the tumor and the pharmacokinetics of the process after injection of C_{60}/HP-β-CyD nanoparticles are currently under investigation in our laboratory.

Conflict of Interests

The authors declare that there is no conflict of interests regarding the publication of this paper.

Acknowledgments

This paper was funded by the Deanship of Scientific Research (DSR), King Abdulaziz University, under Grant no. 1-13-1432/HiCi. The authors, therefore, acknowledge with thanks DSR technical and financial support. This work was partly supported by JSPS KAKENHI Grant no. 23790062.

References

[1] A. P. Castano, T. N. Demidova, and M. R. Hamblin, "Mechanisms in photodynamic therapy. Part one: photosensitizers, photochemistry and cellular localization," *Photodiagnosis and Photodynamic Therapy*, vol. 1, no. 4, pp. 279–293, 2004.

[2] A. P. Castano, T. N. Demidova, and M. R. Hamblin, "Mechanisms in photodynamic therapy. Part two: cellular signaling, cell metabolism and modes of cell death," *Photodiagnosis and Photodynamic Therapy*, vol. 2, no. 1, pp. 1–23, 2005.

[3] A. P. Castano, T. N. Demidova, and M. R. Hamblin, "Mechanisms in photodynamic therapy. Part three: photosensitizer pharmacokinetics, biodistribution, tumor localization and modes of tumor destruction," *Photodiagnosis and Photodynamic Therapy*, vol. 2, no. 2, pp. 91–106, 2005.

[4] T. J. Dougherty and S. L. Marcus, "Photodynamic therapy," *European Journal of Cancer A*, vol. 28, no. 10, pp. 1734–1742, 1992.

[5] S. Yano, S. Hirohara, M. Obata et al., "Current states and future views in photodynamic therapy," *Journal of Photochemistry and Photobiology C*, vol. 12, no. 1, pp. 46–67, 2011.

[6] R. Bakry, R. M. Vallant, M. Najam-ul-Haq et al., "Medicinal applications of fullerenes," *International Journal of Nanomedicine*, vol. 2, no. 4, pp. 639–649, 2007.

[7] A. W. Jensen, S. R. Wilson, and D. I. Schuster, "Biological applications of fullerenes," *Bioorganic and Medicinal Chemistry*, vol. 4, no. 6, pp. 767–779, 1996.

[8] R. Partha and J. L. Conyers, "Biomedical applications of functionalized fullerene-based nanomaterials," *International Journal of Nanomedicine*, vol. 4, pp. 261–275, 2009.

[9] M. R. Hamblin, P. Mroz, G. P. Tegos et al., "Photodynamic therapy with fullerenes," in *Fullerene Research Advances*, C. N. Kramer, Ed., chapter 1, pp. 1–31, Nova Science, New York, NY, USA, 2007.

[10] J. W. Arbogast, A. P. Darmanyan, C. S. Foote et al., "Photophysical properties of C_{60}," *Journal of Physical Chemistry*, vol. 95, no. 1, pp. 11–12, 1991.

[11] T. Nagano, K. Arakane, A. Ryu et al., "Comparison of singlet oxygen production efficiency of C_{60} with other photosensitizers, based on 1268 nm emission," *Chemical and Pharmaceutical Bulletin*, vol. 42, no. 11, pp. 2291–2294, 1994.

[12] J. W. Arbogast, C. S. Foote, and M. Kao, "Electron transfer to triplet fullerene C_{60}," *Journal of the American Chemical Society*, vol. 114, no. 6, pp. 2277–2279, 1992.

[13] D. Iohara, F. Hirayama, K. Higashi, K. Yamamoto, and K. Uekama, "Formation of stable hydrophilic C_{60} nanoparticles by 2-hydroxypropyl-β-cyclodextrin," *Molecular Pharmaceutics*, vol. 8, no. 4, pp. 1276–1284, 2011.

[14] D. Iohara, M. Hiratsuka, F. Hirayama et al., "Evaluation of photodynamic activity of C_{60}/2-hydroxypropyl-β-cyclodextrin nanoparticles," *Journal of Pharmaceutical Sciences*, vol. 101, no. 9, pp. 3390–3397, 2012.

[15] M. Triesscheijn, P. Baas, J. H. M. Schellens, and F. A. Stewart, "Photodynamic therapy in oncology," *Oncologist*, vol. 11, no. 9, pp. 1034–1044, 2006.

[16] D. Heymann, "Solubility of fullerenes C_{60} and C_{70} in seven normal alcohols and their deduced solubility in water," *Fullerene Science and Technology*, vol. 4, no. 3, pp. 509–515, 1996.

[17] R. S. Ruoff, D. S. Tse, R. Malhotra, and D. C. Lorents, "Solubility of C_{60} in a variety of solvents," *Journal of Physical Chemistry*, vol. 97, no. 13, pp. 3379–3383, 1993.

[18] A. Ikeda, Y. Doi, M. Hashizume, J.-I. Kikuchi, and T. Konishi, "An extremely effective DNA photocleavage utilizing functionalized liposomes with a fullerene-enriched lipid bilayer," *Journal of the American Chemical Society*, vol. 129, no. 14, pp. 4140–4141, 2007.

[19] H. Tokuyama, S. Yamago, E. Nakamura, T. Shiraki, and Y. Sugiura, "Photoinduced biochemical activity of fullerene carboxylic acid," *Journal of the American Chemical Society*, vol. 115, no. 17, pp. 7918–7919, 1993.

[20] Y. Yamakoshi, N. Umezawa, A. Ryu et al., "Active oxygen species generated from photoexcited fullerene (C_{60}) as potential medicines: $O_2^{\cdot -}$ versus $^1O_2$," *Journal of the American Chemical Society*, vol. 125, no. 42, pp. 12803–12809, 2003.

[21] G. R. Buettner, "Spin Trapping: ESR parameters of spin adducts 1474 1528V," *Free Radical Biology and Medicine*, vol. 3, no. 4, pp. 259–303, 1987.

[22] M. R. Detty, S. L. Gibson, and S. J. Wagner, "Current clinical and preclinical photosensitizers for use in photodynamic therapy," *Journal of Medicinal Chemistry*, vol. 47, no. 16, pp. 3897–3915, 2004.

[23] J. M. Fernandez, M. D. Bilgin, and L. I. Grossweiner, "Singlet oxygen generation by photodynamic agents," *Journal of Photochemistry and Photobiology B*, vol. 37, no. 1-2, pp. 131–140, 1997.

[24] L. Jaesang, Y. Yamakoshi, J. B. Hughes, and K. Jae-Hong, "Mechanism of C photoreactivity in water: fate of triplet state and radical anion and production of reactive oxygen species," *Environmental Science and Technology*, vol. 42, no. 9, pp. 3459–3464, 2008.

[25] B. Krammer and K. Plaetzer, "ALA and its clinical impact, from bench to bedside," *Photochemical and Photobiological Sciences*, vol. 7, no. 3, pp. 283–289, 2008.

[26] T. J. Dougherty, C. J. Gomer, B. W. Henderson et al., "Photodynamic therapy," *Journal of the National Cancer Institute*, vol. 90, no. 12, pp. 889–905, 1998.

[27] J. Zilberstein, A. Bromberg, A. Frantz et al., "Light-dependent oxygen consumption in bacteriochlorophyll-serine-treated melanoma tumors: online determination using a tissue-inserted oxygen microsensor," *Photochemistry and Photobiology*, vol. 65, no. 6, pp. 1012–1019, 1997.

[28] S. Mimura, T. Otani, and S. Okuda, "Photodynamic therapy for superficial esophageal cancer using an excimer dye laser," *Diagnostic and Therapeutic Endoscopy*, vol. 1, no. 2, pp. 99–105, 1994.